The passage of Ca^{2+} and fluorescent markers between the sperm and egg after fusion in the mouse

Keith T. Jones[1],[*],[‡], Christian Soeller[2] and Mark B. Cannell[2],[*]

[1]Department of Anatomy and Developmental Biology, University College, London WC1E 6BT, UK
[2]Department of Pharmacology, St George's Hospital Medical School, London SW17 0RE, UK, and Department of Physiology, University of Auckland, Grafton Street, Auckland 1, New Zealand
[‡]Present address: Department of Physiological Sciences, The Medical School, Framlington Place, University of Newcastle upon Tyne, Newcastle upon Tyne, NE2 4HH, UK
[*]Authors for correspondence

SUMMARY

Mouse sperm-egg fusion was examined using two-photon and confocal microscopy. A delay of several minutes occurred between the first observable event of fusion (which was the diffusion of Ca^{2+}-sensitive dyes from egg into sperm) and any change in egg cytoplasmic Ca^{2+}. When indo-1 dextran was used to obtain ratiometric two-photon images, there was no detectable local increase in egg cytoplasmic Ca^{2+} near the site of sperm fusion. However, the sperm underwent a Ca^{2+} transient which appeared to be coincident with the egg cytoplasm Ca^{2+} transient, which suggested that there was a high permeability pathway for Ca^{2+} between egg and sperm. To exclude this pathway from providing trigger Ca^{2+} for the egg transient, we reduced bathing $[Ca^{2+}]$ to approx. 18 μM and 13nM (with EGTA). In these conditions the first egg Ca^{2+} transient was not prevented, which makes an obligatory role for extracellular Ca^{2+} in the initiation of the egg Ca^{2+} transient unlikely.

Both FITC-albumin (70 kDa) and 10 kDa dextran-linked Ca^{2+} indicators were able to diffuse into the sperm from the egg. In addition, phycoerythrin (240 kDa) rapidly diffused into the sperm shortly after fusion (but before any changes in Ca^{2+} occurred). This suggests that the 'pore(s)' that form during sperm-egg fusion must be at least 8 nm in diameter. These data are compatible with the idea that a diffusible sperm protein could trigger the observed changes in intracellular Ca^{2+} in the egg, but do not exclude the possibility that other second messengers are generated during sperm-egg fusion.

Key words: Sperm, Egg, Fertilization, Ca^{2+}, Confocal imaging, Mouse

INTRODUCTION

Activation of the egg at fertilization in a wide variety of species is triggered by changes in the intracellular Ca^{2+} concentration (Zucker et al., 1978; Kline 1988; Kline and Kline, 1992; McDougall et al., 1995). However, the mechanism employed by the sperm to trigger Ca^{2+} release remains uncertain (reviewed in Jaffe, 1991; Whitaker and Swann, 1993; Schultz and Kopf, 1995; Swann and Lai, 1997). Three models have been proposed to explain the rise in Ca^{2+} termed the 'conduit', 'contact' and 'content' models (Jaffe, 1991).

The 'conduit' model proposes that the sperm acts as a channel to allow Ca^{2+} from the extracellular medium to enter the egg, thereby overloading stores and causing Ca^{2+} release (Jaffe, 1991). Alternatively, sperm may be a source of Ca^{2+}, an idea which was first proposed in the 'Ca^{2+} -bomb' hypothesis (Jaffe, 1980, 1983) and which would be favoured by the increase in mammalian sperm Ca^{2+} during capacitation and acrosome reaction (Visconti and Kopf, 1998; Florman et al., 1998; for review see Yanagimachi, 1994). In frog and fish eggs, further support for this idea is provided by the observation that a single Ca^{2+} wave is

observed at fertilization which is mimicked by surface membrane damage (Gilkey, 1983; Kubota et al., 1987). This is not the case for sea urchin (Swann and Whitaker, 1986) although Ca^{2+} chelators and La^{3+} block egg activation (Creton and Jaffe, 1995) (note that the latter might also be considered supportive of the 'conduit' model -see above). In mammalian eggs, there are a series of low frequency transients (Cuthbertson and Cobbold, 1985) which are not produced by Ca^{2+} injection or electroporation (McNiven et al., 1988; Fissore and Robl, 1992; Sun et al., 1992; Collas et al., 1993; Ozil and Swann, 1995). In any case, such interventions may not mimic the behaviour of a slow Ca^{2+} leak from the sperm (Jaffe, 1990; Creton and Jaffe, 1995).

The 'contact' model proposes that sperm bind to the plasma membrane to activate phospholipase C (PLC) and produce inositol trisphosphate (IP_3). The involvement of this pathway is suggested by the oscillations produced by IP_3 injection (Swann et al., 1989; Jones and Whittingham, 1996) and the block of sperm-induced oscillations by PLC inhibition (DuPont et al., 1996). Furthermore, an antibody to the IP_3 receptor blocks sperm's ability to release Ca^{2+} (Miyazaki et al.,

1992). However, there has been no report of a sperm-derived ligand which interacts with the egg membrane to cause Ca^{2+} oscillations in mammals.

The 'content' model proposes that a sperm component (sperm factor) is responsible for Ca^{2+} release in the egg. At present, there are three possible candidates. (1) Glucosamine-6-phosphate deaminase, a protein composed of 33 kDa monomers (Parrington et al., 1996); however the recombinant protein has no Ca^{2+} releasing activity (Wolosker et al., 1998). (2) A truncated form of c-kit (tr-kit), a 23 kDa protein which causes Ca^{2+}-dependent egg activation (Sette et al., 1997). (3) Calicin, a 60 kDa protein found in the 'calyx' (Kimura et al., 1998). Deaminases have been reported to be hexameric (Calcagno et al., 1984) and tr-kit yields a 48 kDa product (Albanesi et al., 1996). Therefore, current 'content' models require the formation of large pores but only 10 kDa dextrans have been shown to pass between egg and sperm before the Ca^{2+} transient occurs (Lawrence et al., 1997).

Using two-photon (TPM) and confocal microscopy we have measured Ca^{2+} changes which occur in mouse eggs around the time of sperm fusion. We show that the pores which form after sperm fusion allow very high molecular weight proteins to pass between egg and sperm – as required by the 'content' model. No evidence was found for a role of extracellular Ca^{2+} in initiation of the first Ca^{2+} transient.

MATERIALS AND METHODS

Gamete collection

4- to 8-week old female F_1 hybrid mice of B6CB (C57Bl/6JLac × CBA/CaLac), were superovulated by serial injection of 7.5 i.u. pregnant mares' serum gonadotrophin and 5 i.u. human chorionic gonadotrophin (hCG) given 48 hours apart. Eggs were collected 13-14 hours post-hCG injection in medium M2 (Fulton and Whittingham, 1978; Quinn et al., 1982). The cumulus cells were removed by a brief incubation in hyaluronidase (0.3 mg/ml). Sperm were collected from known fertile F_1 hybrid mice and capacitated for at least 2 hours in medium T6 at a concentration of 1-2×10^5 sperm/ml (Quinn et al., 1982).

Dye microinjection

Eggs were microinjected as described previously (Jones et al., 1995) with Ca^{2+}-green dextran (10 kDa), or indo-1 dextran (10 kDa) which were obtained from Molecular Probes (Eugene, OR), to final concentrations of 10-30 μM in the egg cytosol. In other systems, pore sizes have been measured using fluorescent markers of varying size (e.g., Wyke et al., 1980; Sauer et al., 1991) and we have used this approach using phycoerythrin (240 kDa) and FITC-albumin (70 kDa) which were obtained from Sigma (St. Louis, MO). All fluorescent probes were dissolved in 120 mM KCl, 20 mM Hepes, pH 7.5 for injection. The fluorescent proteins were washed extensively overnight with several ten-fold dilutions in KCl injection buffer using 30 kDa Centricon cut-off filters and centrifugation at 5000 g (Amicon, Beverly, MA) (to remove lower molecular weight contaminants). Eggs were placed in M2 under oil on the stage of a Nikon Diaphot inverted microscope. Borosilicate glass capillaries (1.5 mm outer diameter × 0.86 mm inner diameter) with an internal filament (Clark Electromedical Instruments, UK) were pulled on a vertical pipette puller (David Kopf Instruments, CA) and the tips broken on cotton wool to give a pipette resistance of 10-50 MΩ (when filled with the injection solution. Micropipettes were inserted into cells by overcompensation of negative

capacitance on an electrophysiological amplifier used to monitor membrane potential. A precise, bolus, injection corresponding to 5% of the total cell volume was achieved by using a Pneumatic PicoPump (World Precision Instruments) with success rates of >95%. To allow time for diffusion of dye within the eggs, a period of at least 20 minutes from the time of microinjection was allowed and the eggs were stored in M2 medium at 37°C for not more than 4 hours.

Preparation of eggs for recording

The injected eggs had their zonae removed by a brief (10 seconds) incubation in acid Tyrode's solution. Eggs were then immediately transferred to a heated chamber (Intracel) at 37°C containing 500 μl of M2 without bovine serum albumin (BSA). The eggs were allowed to attach to the glass base in BSA-free M2 before the addition of 500 μl of M2 containing 14 mg/ml V BSA. In all experiments, complete diffusion of injected dye was confirmed by the uniform distribution of fluorescence throughout the entire egg before adding any sperm to the solution. To record Ca^{2+} changes at fertilization 10 μl of capacitated sperm suspension were added to the chamber and as soon as sperm reached the egg (as observed by conventional light microscopy), fluorescence imaging was started.

Imaging

A modified Zeiss LSM 410 confocal microscope (Zeiss, Oberkochem) was used which had an Ar-ion and a Ti:Sapphire (Coherent, Santa Clara, CA) laser as light sources. For two-photon imaging, the Ti:Sapphire laser was used with the emission pinhole fully open and excitation wavelength of 690 nm for Indo-1 or 850 nm for Ca^{2+}-green. Pulse lengths were less than 100 fs at the sample (see Soeller and Cannell, 1996 for further details). For conventional confocal imaging, the pinhole diameter was set to <1.2 Airey units which provided a similar resolution to that obtained when using 2-photon excitation and a fully open pinhole (approx. $0.35 × 0.35 × 0.7$ μm x, y and z respectively). For ratio imaging of indo-1 a 450 nm long pass filter was used to split the emitted light. Ratios were calculated as the ratio of intensity in the long wavelength channel ($\lambda > 450$ nm) and short wavelength intensity ($\lambda < 450$ nm). A 40× 1.2 N.A. water immersion objective was used and this objective was heated to 37°C by a warming coil fitted to the objective body. Excitation and emission filters were custom filters manufactured by Chroma (Brattleboro, VT) to the authors' specifications. Normally, imaging was carried out at pixel dwell times of approx. 2 μseconds and for fast scanning only 10 scan lines were acquired to provide images of a narrow part of the cell at 100 frames/second. The host computer memory for the LSM410 was increased to 32 Mbyte to allow rapid storage of large numbers of images (or in some cases images were written to magnetic disk via cache memory). Image processing and analysis was carried out using custom routines written in IDL (Research Systems, Boulder CO) running on Silicon Graphics Workstations (Mountain View, CA). Long term image archive was provided by 1.2 GByte magneto-optical disks supported by a Silicon Graphics file server.

RESULTS

In all experiments (n>30), eggs were microinjected with either dextran-linked indo-1 or dextran-linked Ca^{2+}-green. Following addition of sperm to the heated chamber containing eggs, no detectable sperm autofluorescence was observed. However, after attachment of sperm to an egg, the fluorescence in the attached sperm increased until it became at least as fluorescent as the egg cytoplasm (Fig. 1A,B). The period between sperm addition and attachment to the egg (as observed by

conventional light microscopy) was variable, but was not less than two minutes. This delay was due to the time taken for sperm to swim to the egg from their (more distant) site of addition in the chamber. The time interval between sperm attachment and an increase in sperm fluorescence was also variable, with some sperm it was a few tens of seconds while in others it took several minutes. Sperm fluorescence always developed in both the head and the mid piece of the tail, but this observation could not be confirmed at more distal tail pieces because of egg movement (due to other unfused sperm). In all experiments described here, only eggs with a single fused sperm were analyzed, although in a very few cases polyspermy was observed. After a variable delay (1-5 minutes), eggs produced a transient increase in cytoplasmic Ca^{2+} (Fig. 1C). The increase in Ca^{2+} propagated across the cell in about 2 seconds until the entire cytoplasmic Ca^{2+} level was elevated (see below and Fig. 1C). At least a part of the variation in the time taken to produce a Ca^{2+} transient after sperm fusion was

probably due to the time taken to find the attached sperm which was complicated by the narrow depth of focus of the microscope.

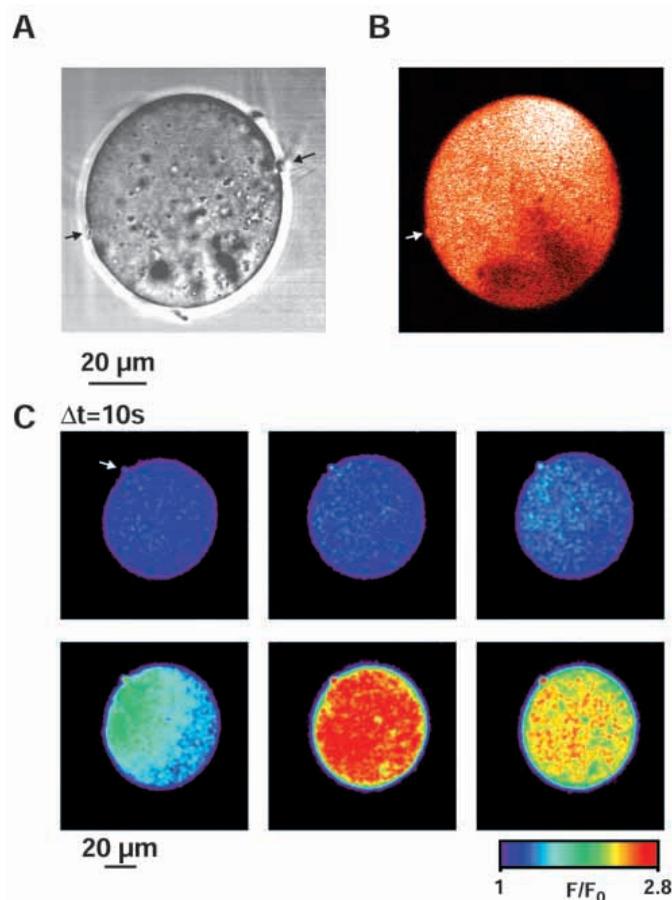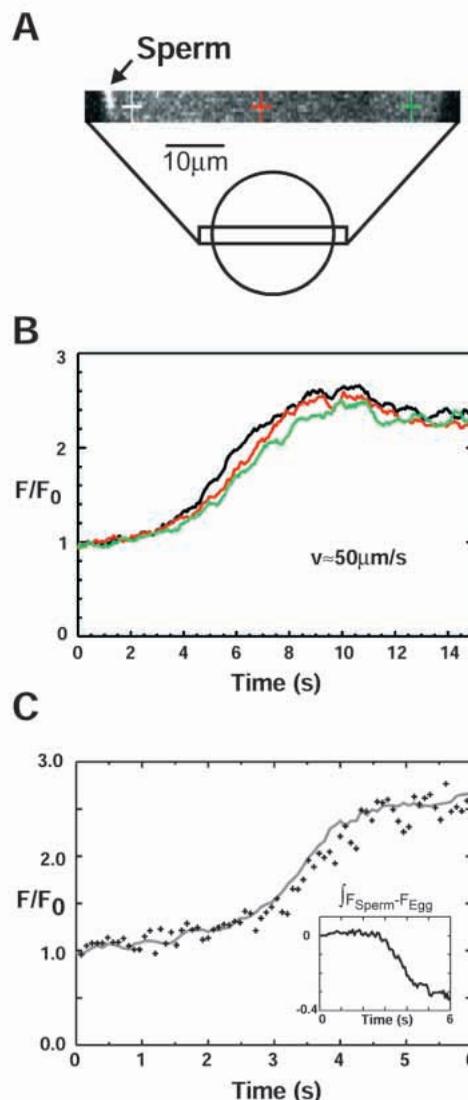The time course of propagation of the increase in

Fig. 1. Visualization of sperm-egg fusion and fertilization wave. (A) A transmitted light image of a mouse egg injected with calcium green-1 dextran (10 kDa) to which two sperm (at arrows) are attached. (B) A section through the same egg using two-photon microscopy is shown. Note that only one of the sperm heads visible in A can be seen (at the arrow) in this fluorescence image and that this sperm must have formed a permeability pathway to the egg cytosol whereas the other sperm did not. The sequence of images in C shows the propagation of the Ca^{2+} transient (fertilization wave) which follows sperm fusion. The sperm head is clearly seen at the arrow.

Fig. 2. Time course of the first fluorescence transient after sperm fusion at high temporal resolution. After locating a fused sperm by Ca Green-1 fluorescence imaging (compare Fig. 1), the area of observation was reduced to 9 scan lines as indicated in A which allowed acquisition of 100 images/second. In B the normalized fluorescence transient at three locations (marked by crosses in A) is shown. The fluorescence increases first in the cytosol near the sperm (white cross and black line). From the delay in the fluorescence time course to that at the center (red) and at the far edge (green) of the egg cytosol a wave propagation speed of approx. 50 mm/second was estimated. C shows the time course of normalized fluorescence in the sperm head (crosses) and the egg cytosol approx. 1 μm from the sperm (solid line). These data suggest that the transient in the sperm head lags behind that in the adjacent cytosol. This point is clarified in the inset, where the integral of the difference in normalized fluorescence at these two sites is plotted as a function of time. Note that the running integral is initially zero and then becomes negative which indicates that the sperm fluorescence transient *follows* the egg cytosolic transient.

fluorescence across the egg is examined in Fig. 2. By limiting the region that was examined to just a few lines (Fig. 2A) it was possible to acquire images at 100 frames/second. The time course of fluorescence change in the egg cytoplasm near the sperm and at two more distant sites (indicated in Fig. 2A) are shown in Fig. 2B. At all three sites, fluorescence increased initially exponentially before reaching a peak in about 6 seconds. However, the signal from the site distal to the sperm (green trace) was delayed by about 1-2 seconds relative to the site proximal to the sperm. These data are consistent with the egg cytoplasm behaving as an excitable medium with a wave being initiated near the site of sperm fusion. The propagation velocity of the Ca^{2+} wave across the cytoplasm was approx. 50 µm/second and was consistent with that previously reported for the mouse (47.5 ± 6.06 µm/second; Cheek et al., 1993) but faster than the 16-28 µm/second found in hamster (Miyazaki et al., 1986). Furthermore the fact that the cytoplasm near the sperm responded first would be consistent with the idea that sperm initiates the Ca^{2+} wave from the site of sperm fusion (Miyazaki et al., 1986; Cheek et al., 1993).

If Ca^{2+} influx via the sperm provided 'trigger' Ca^{2+} for Ca^{2+} wave initiation, the cytoplasmic Ca^{2+} level in the sperm should increase before the egg or be higher than that in the egg. The first possibility is examined in Fig. 2C which shows the time course of normalized fluorescence change in the sperm and egg cytoplasm near the site of sperm fusion. Although the change in normalized fluorescence from the egg and sperm had a similar amplitude and time course, there was no evidence to support the idea that the sperm Ca^{2+} changes might precede those of the egg. In fact, the sperm signal appeared to lag behind the egg cytoplasm signal by about 0.2 seconds (Fig. 2C). In 3 additional experiments, we could not detect any evidence for a delay between the time course of fluorescence change in the sperm and the egg cytoplasm near the sperm. Although many other studies have shown that Ca^{2+} waves develop after fusion (e.g. Miyazaki et al., 1986), these data are the first demonstration that the sperm also undergoes a Ca^{2+} transient coincident with the initiation of the egg wave. However, the absolute level of fluorescence from the sperm was quite different from that in the egg cytoplasm which would complicate the interpretation of these data (see Fig. 2A). To overcome this problem, dextran-linked indo-1 was used with the fluorescence being recorded at two wavelengths to allow calculation of ratio images (Fig. 3). In Fig. 3A the Ca^{2+} increase in both the sperm and egg can be seen and it is apparent that the amplitude of the change in Ca^{2+} in both the sperm and egg are comparable. Although the signal-to-noise ratio in the indo-1 ratio images was lower and it was not possible to perform a detailed analysis of the kinetics of the Ca^{2+} change, when taken together, the indo-1 and Ca^{2+}-green experiments showed that the Ca^{2+} changes in the sperm head had (essentially) the same amplitude and time course as the changes in the egg cytoplasm near the site of sperm fusion. Nevertheless, the absolute indo-1 ratio in the sperm was slightly different from that in the egg, an effect that appeared to be related to the fact that all of the fluorescent indicators (see Figs 4A, 5B,C below also) produced larger signals in the sperm head than in the egg. Even when high signal to noise ratio images were obtained (Fig. 3B) a small difference

in Indo-1 ratio remained which did not exclude the possibility that the sperm might be providing Ca^{2+} to the egg.

In cardiac muscle it has been suggested that it is also possible for a Ca^{2+} wave to be initiated by a low amplitude Ca^{2+} influx to induce a local 'Ca^{2+} overload' resulting from an increase in cytoplasmic Ca^{2+} being taken up by intracellular stores which then become unstable and initiate wave generation (Fabiato, 1985; Wier and Blatter, 1991; see also Takamatsu and Wier, 1990 and Cheng et al., 1996). In this case, a marked difference between the levels of Ca^{2+} in the sperm and egg (as well as their time course) might not be detected if the permeability of the site of sperm fusion was high (see below). The induction of Ca^{2+} overload in this way should be detectable as a local increase in cytoplasmic Ca^{2+} near the Ca^{2+} source -the sperm. However, the high resolution indo-1 image in Fig. 3B does not support the idea that the egg cytoplasmic Ca^{2+} level near the sperm was higher than at more distant sites. This view was supported by quantification of the ratio levels from the regions marked 1 and 2 in Fig. 3C. The fluorescence ratio in box 1 was 0.54 ± 0.04 and in box 2 was 0.53 ± 0.03 (mean ± s.d., $n=1225$ pixels). These regions were not therefore significantly different ($P<0.01$). Similar results were obtained in 3 additional experiments.

Nevertheless, we considered that these data did not rule out the possibility that a very small Ca^{2+} influx from the sperm ('conduit model') might remain undetected, and given the problems in accurate interpretation of indo-1 ratio images from different cellular compartments we decided to manipulate extracellular Ca^{2+} to minimize any possible Ca^{2+} influx from the sperm. Eggs placed in a nominally Ca^{2+} free medium also showed a transient increase in intracellular Ca^{2+} after sperm fusion (Fig. 4A). Since the T6 medium used to capacitate sperm (Quinn et al., 1982) contained 1.78 mM Ca^{2+} the dilution of the sperm solution by the solution in the chamber would have increased the extracellular Ca^{2+} level to about 18 µM. Although this low Ca^{2+} should have reduced the possible Ca^{2+} influx into the sperm and egg by more than an order of magnitude it cannot exclude the possibility that some Ca^{2+} influx might still occur. To further reduce Ca^{2+} levels a Ca^{2+}-free bathing medium containing 100 µM EGTA was used. In this solution, the increase in extracellular Ca^{2+} concentration brought about by sperm addition should have been 13 nM (Maxchelator Shareware v4.63). This low level of extracellular Ca^{2+} (see Discussion) should have reversed any gradient of Ca^{2+} from sperm to egg and thereby prevented any calcium influx via the sperm. Although sperm rapidly lost motility in this solution, in 5 out of 8 eggs fusion and a Ca^{2+} transient occurred (as illustrated in Fig. 4B). From these experiments, it follows that an influx of extracellular Ca^{2+} is unlikely to be involved in the initiation of the fertilization Ca^{2+} transient in mouse.

As noted above, the fact that the sperm undergoes a Ca^{2+} transient coincident with the egg transient shows that a significant permeability pathway develops shortly after sperm fusion. Since the fluorescent Ca^{2+} indicators used ($\leq$10 kDa) could readily diffuse into the sperm before the initiation of a Ca^{2+} wave, these data suggest that moderate molecular weight substances can diffuse between the sperm and egg (Lawrence et al., 1997), as required for the 'content' model (see Introduction). In conjunction with this point, we

verified that diffusion of dye from the egg into the sperm was fast by attempting to selectively bleach the sperm fluorescence. However, attempts to bleach sperm fluorescence by repetitive scanning failed (not shown). This was despite the fact that independent tests showed that fluorochromes could be photobleached when immobilized in gels (Cannell and Soeller, 1997) or in small drops of saline at similar excitation powers. Experiments with even higher molecular weight indicators were performed to estimate the minimum size of the pores associated with this permeability pathway. The first series of experiments used dextran-linked indo-1 as a fusion marker for eggs which also contained FITC labeled albumin (70 kDa). Sperm-egg fusion was detected by monitoring fluorescence of dextran-linked indo-1 in the sperm head by two-photon excitation at 710 nm. In this mode the majority of fluorescence is due to indo-1 (Fig. 5A). When fusion was detected, the excitation wavelength was switched to 488 nm and FITC-albumin fluorescence was measured at 520 nm in the conventional confocal mode of the microscope. The lack of cross-talk between indo-1 and FITC signals was confirmed in eggs that were injected with either indo-1 or FITC-albumin (Fig. 5A). Fig. 5B shows an egg labeled with both indo-1 dextran and FITC-albumin, and it is apparent that both markers readily entered the sperm head. Furthermore, the relative intensity of the FITC-albumin signal between the sperm and egg was as large as the relative sperm-egg indo-1 dextran signal. This suggests that the delay in the passage of FITC-albumin into the sperm must have been comparable to that of the indo-1 dextran and certainly less than the time taken to switch microscope excitation wavelengths (about 5 seconds). We conclude that the pores linking the cytoplasm of the egg and sperm are not only large but also develop rapidly during (or after) sperm-egg fusion.

To further examine the size of the pores linking sperm and egg we used phycoerythrin (240 kDa) whose fluorescence (maximum at 575 nm) is an intrinsic property of the molecule. As shown in Fig. 5C, phycoerythrin also entered the egg cytoplasm at the same time as indo-1 dextran. Therefore, diffusion of these globular protein markers suggest that pores >8 nm in diameter (see Discussion) form rapidly after sperm fusion. Such large pores would allow Ca^{2+} changes in the egg cytoplasm to pass rapidly into the sperm and can explain why the sperm undergoes a synchronous Ca^{2+} transient with the egg (see above). In addition, such pores would permit high molecular weight substances to pass from the sperm to the egg as required for the 'content' model.

DISCUSSION

The present experiments describe observations made on mouse eggs following sperm fusion using a two-photon/confocal imaging system (Soeller and Cannell, 1996). Sperm-egg fusion was observed by the transfer of markers (some of which were used for Ca^{2+} measurement) from the egg into the sperm head. From the time of (measurable) fusion until the first sperm-egg Ca^{2+} transient there was a distinct delay, the latent period, that was at least 1 minute. These observations are in agreement with a recent detailed study of the length of the latent period between sperm fusion and Ca^{2+}

changes in the mouse egg (Lawrence et al., 1997). We have excluded both the Ca^{2+} 'conduit model' and the 'Ca^{2+} bomb' hypothesis for the initiation of the first Ca^{2+} rise by examining local Ca^{2+} changes in the sperm and egg as well as by manipulation of extracellular Ca^{2+} levels. In addition, we found that large diameter pores, which would be obligatory for the 'content' model for egg activation, form before any detectable increase in Ca^{2+}.

Two-photon imaging of sperm and eggs

In a small number of eggs (<5%) there was no observable sperm fusion even though the egg was surrounded by many sperm. In such eggs there was never a spontaneous increase in Ca^{2+}. Similarly, even in eggs that underwent sperm fusion, there was no spontaneous Ca^{2+} increase in eggs before the fusion event. Therefore, the Ca^{2+} changes that were recorded could not be explained by an artifact associated with two-photon imaging.

The obvious explanation for the increase in sperm fluorescence after sperm-egg fusion is that the fluorescent indicators diffused from the egg cytoplasm into the sperm. In addition, the increase in sperm fluorescence occurred at the emission wavelength of the injected fluorochrome regardless of which fluorochrome was used. This observation makes it highly unlikely that some change in an intrinsic sperm fluorochrome (which would have a unique emission spectrum) was responsible for the development of sperm fluorescence. Our inability to selectively photobleach sperm fluorescence showed that the permeability of the pathway from the sperm to the egg must have been large enough to ensure that diffusion of fresh fluorochrome from the egg (which acts as a large reservoir) prevented significant reduction in fluorochrome levels in the sperm. This view is supported by the 'pore sizing' experiments with FITC-albumin and phycoerythrin which suggest that the sperm cytoplasm is readily accessed from the egg cytoplasm by high molecular weight substances.

Role of extracellular Ca^{2+} at fusion and during the latent period

The two-photon imaging facilitated the use of ratiometric dyes for Ca^{2+} recording by reducing fluorochrome photobleaching. This reduction in photobleaching allowed continuous imaging of the egg while attempting to locate the plane of sperm fusion (as well as during the time which elapsed after sperm addition to the experimental chamber). It was also possible to obtain high quality ratio images (Fig. 3) of the area surrounding the site of sperm fusion and these images showed no detectable local elevation in cytoplasmic Ca^{2+} before the initiation of the Ca^{2+} wave. As noted above, this observation makes it unlikely that the sperm supplies a Ca^{2+} trigger that initiates the Ca^{2+} wave in mouse. Similarly, no measurable Mn^{2+} influx occurs in mouse eggs before the initiation of sperm-induced Ca^{2+} oscillations (McGuiness et al., 1996). Although in sea urchin eggs, addition of La^{3+} or Ca^{2+} chelators block egg activation (Creton and Jaffe, 1995), these apparently conflicting results may be due to non-specific effects of La^{3+} as well as the problematic gradual loss of sperm motility in low Ca^{2+} solutions.

When Ca^{2+} was omitted from the extracellular medium and
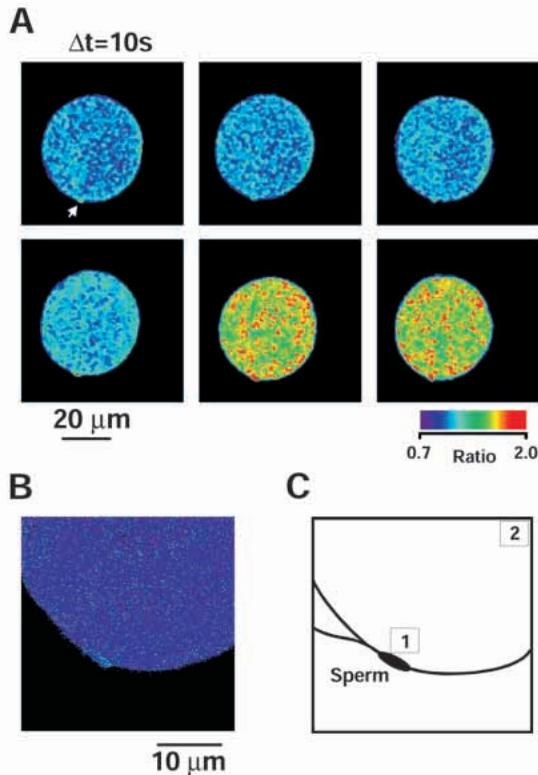
Fig. 3. Two-photon imaging of indo-1 fluorescence. A shows a sequence of ratio images of indo-1 fluorescence (two-photon excitation at 690 nm) during the first calcium transient after sperm fusion. Note that the amplitude of ratio changes of the sperm (arrow) and egg cytosol are comparable. (B) High resolution indo-1 ratio image showing sperm head and cytosol (see schematic drawing in C). The fluorescence ratio in an area of the cytosol close to the sperm immediately after sperm fusion and before the first calcium transient (box 1, R=0.54±0.04) was not significantly different from that in a region distant from the sperm (box 2, R=0.53±0.03, mean (s.d. n=1225 pixels).

Fig. 4. Egg Ca^{2+} transients in nominally calcium-free and EGTA-buffered external solutions. (A) A Ca^{2+} transient which occurred after sperm fusion in a nominally calcium-free solution (see text). The site of sperm fusion is indicated by an arrow. In B the fluorescence transient in an egg can be seen in a solution containing 100 µM EGTA (to buffer residual calcium to approx. 13 nM).

100 µM EGTA added, sperm viability was quickly affected so that the majority of sperm were immotile within about 10 minutes. This result is in agreement with detailed studies of sperm viability in various Ca^{2+} buffers (Yanagimachi, 1978; Heffner and Storey, 1981). However in >50% of eggs, sperm fusion still occurred and the first Ca^{2+} wave propagated in the same way as observed in normal Ca^{2+}-containing media. These results appear to exclude the possibility that extracellular Ca^{2+} or Ca^{2+} within the sperm head produces the first Ca^{2+} transient in the egg. In addition, it is clear that normal extracellular Ca^{2+} levels are not required for sperm-egg fusion (beyond that being associated with the maintenance of sperm motility). In agreement with this result, in sea urchin, human, guinea pig and mouse, sperm fusion has been achieved in Mg^{2+}-containing media with no added Ca^{2+} (Yanagimachi, 1978; Schmidt et al., 1982; Conover and Gwatkin, 1988). It should be noted that M2 medium contains 1.19 mM Mg^{2+} (Quinn et al., 1982), so our results are fully consistent with the lack of an obligatory role of Ca^{2+} in sperm-egg fusion.

It has been argued that the transient elevation of Ca^{2+} associated with sperm addition could preclude exclusion of the
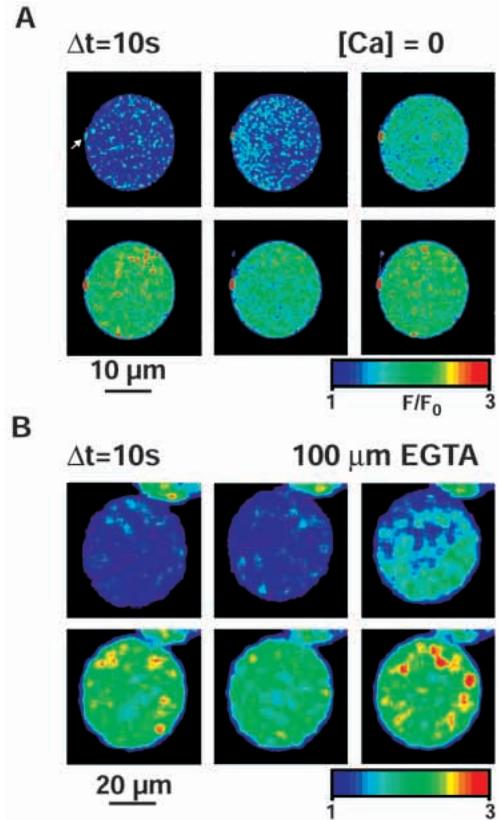
'Ca^{2+} bomb' and 'Ca^{2+} conduit' hypotheses (Jaffe, 1990). However, we avoided this complication by adding sperm several millimeters from the egg in an EGTA containing medium. If no mixing occurred, the free Ca^{2+} at the egg would have been even lower than that calculated (13 nM). If the egg and sperm solutions were only partially mixed, the free Ca^{2+} at the site of sperm addition would have been higher than 13 nM but that at the egg would still have been less than 13 nM because bulk stirring did not occur and diffusion is slower than swimming sperm.

Sperm-egg fusion in mouse

For the 'content model' to explain the initiation of the Ca^{2+} changes at fertilization, a factor must pass from the sperm to the egg to destabilize the egg Ca^{2+} stores. In agreement with a previous finding (Lawrence et al., 1997), 10 kDa dextran-linked fluorochromes were able to pass from the egg to the sperm. However, the linear nature of dextrans prevents any simple calculation of the size of pores that allow their passage. To overcome this problem we used the globular proteins albumin and phycoerythrin which readily entered the sperm. Use of these proteins allows calculation of a lower limit of the pore size by making two assumptions: first that the proteins are approximately spherical and second that they have a density of
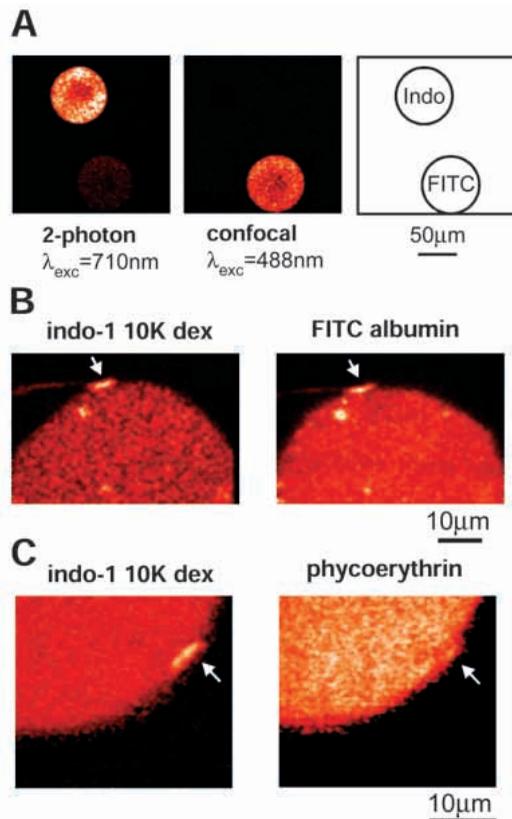
Fig. 5. Optical sizing of pores formed between sperm and egg after sperm fusion. A shows a control experiment in which two eggs were injected with a single label, either indo-1 10 KDa dextran or FITC-labeled albumin. Indo-1 fluorescence was excited (two-photon) at 710 nm and emission recorded at <500 nm while FITC albumin (70 kDa) fluorescence was excited at 488 nm and emission detected >500 nm using the confocal mode of the microscope. Note that no signal from the indo-1 injected egg was detected when FITC fluorescence was monitored. B shows results from an experiment in which the egg was injected with indo-1 10 kDa dextran and FITC albumin simultaneously. The image on the left shows a sperm head (arrow) that has fused with the egg (as indicated by its indo-1 fluorescence emission). Note that the sperm also exhibits FITC albumin fluorescence. The two images in C show the results from a similar experiment (all excitation and detection parameters as in A) except that the egg was injected with indo-1 10 kDa dextran and the fluorescent protein phycoerythrin (240 kDa). Again, as soon as sperm fusion was detected (left image) phycoerythrin fluorescence from the sperm head was also detectable (right image).

1.3 g/cm^3 (Wyke et al., 1980). It follows from the definition of density that the radius of a protein (r) of molecular mass (M), can be estimated as

$$r = \sqrt[3]{3 \cdot M / [4\pi \cdot \mathrm{Av} \cdot 10^{-21} \cdot 1.3]} \text{ nm}$$

where Av is Avogadro's number. With these assumptions, the radius of phycoerythrin is about 4 nm which suggests that the diameter of the pore is >8 nm. This sets a minimum pore size that must be established at the time of fusion in the mouse. In sea urchin, the 'pore' size has been calculated from conductance changes to be approx. 60 nm diameter (Whitaker et al., 1989) which forms at the tip of the acrosomal process

(Longo et al., 1986). Although we have been unable to find a fluorescent marker which did not enter the sperm, there is no *a priori* reason to suppose that such large 'pores' form in mammals since there are obvious differences between invertebrate and mammalian systems (such as the equatorial site of sperm fusion in mammals, Yanagimachi, 1994).

Pore formation

In mammals, the protein(s) which are involved in the formation of the fusion pore are not fully characterized (Myles, 1993; Wolfsberg and White, 1996). Candidates include the PH-30 protein which has two subunits, fertilin α and β of 45-49 kDa and 25-33 kDa respectively (Primakoff et al., 1987; Blobel et al., 1992) which are members of the ADAM family (reviewed in Wolfsberg and White, 1996). Other candidates include the DE protein which has two 37kDa subunits (Rochwerger et al., 1992) but several other candidates have been proposed (reviewed by Myles, 1993). Since the pores appear to form without allowing extracellular Ca^{2+} to enter the cell (as no local Ca^{2+} increase near the site of sperm-egg fusion was detected) this raises a question as to how such large pores might assemble from such smaller candidate proteins.

The mechanism of pore formation at gamete fusion may be analogous to other fusion events such as exocytosis (e.g. see Whitaker and Swann, 1993; Betz and Angleson, 1998). It is unlikely that the pores that we have detected are a single molecule since they would be visible with electron microscopy (note that *E. coli* caseinolytic protease is cylindrical with a pore size of 3.2-3.6 nm and is easily seen in electron micrographs; Flanagan et al., 1995). By analogy with exocytosis, the mouse fusion pore is probably formed by the assembly of protein subunits that are present in both sperm and egg membranes. If this is the case, we suggest that the large quantity of kinetic energy available from sperm motion may power the dislocation of lipid to form a stable pore after protein sub-units in egg and sperm membranes bind. This mechanism would make spontaneous pore fusion extremely unlikely while still allowing motile sperm to achieve fusion. In connection with this point we note that, even when eggs had many sperm attached, no fusion with immotile sperm occurred (not shown).

Conduit, contact or content hypothesis?

The sperm-egg pores detected in this study form a path for high molecular weight substances to enter the egg from the sperm. This finding can therefore be considered to be supportive to the idea that the sperm supplies a factor which destabilizes intracellular Ca^{2+} stores to produce Ca^{2+} transients during fertilization (the 'content' model). Since the present data excludes the 'conduit' model for the initiation of the first Ca^{2+} transient only the 'content' model or the 'contact' model remain candidates. As noted above, simple 'contact' between sperm and egg did not initiate a Ca^{2+} transient unless pore formation also occurred. It follows that a purely 'contact' model seems less likely than the 'content' model at this time.

REFERENCES

Albanesi, C., Geremia, R., Giorgio, M., Dolci, S., Sette, C. and Rossi, P. (1996). A cell- and developmental stage-specific promoter drives the expression of a truncated c-kit during mouse spermatid elongation. *Development* **122**, 1291-1302.

Betz, W. J., Angleson, J. K. (1998). The synaptic vesicle cycle. *Ann. Rev. Physiol.* **60**, 347-363.

Blobel, C. P., Wolfsberg, T. G., Turck, C. W., Myles, D. G., Primakoff, P. and White, J. M. (1992). A potential fusion peptide and an integrin ligand domain in a protein active in sperm-egg fusion. *Nature* **356**, 248-252.

Calcagno, M., Campos, P. J., Mulliert, G. and Suastegui, J. (1984). Purification, molecular and kinetic properties of glucosamine-6-phosphate isomerase (deaminase) from *Escherichia coli. Biochim. Biophys. Acta.* **787**, 165-173.

Cannell, M. B. and Soeller, C. (1997). High resolution imaging using confocal and two-photon molecular excitation microscopy. *Proc. Roy. Micr. Soc.* **32**, 3-8.

Cheek, T. R., McGuinness, O. M., Vincent, C., Moreton, R. B., Berridge, M. J. and Johnson, M. H. (1993). Fertilisation and thimerosal stimulate similar calcium spiking patterns in mouse oocytes but by separate mechanisms. *Development* **119**, 179-189.

Cheng, H., Lederer, M. R., Lederer, W. J. and Cannell, M. B. (1996). Calcium sparks and $[Ca^{2+}]_i$ waves in cardiac myocytes. *Am. J. Physiol.* **270**, C148-C159.

Collas, P., Fissore, R., Robl, J. M., Sullivan, E. J. and Barnes, F. L. (1993). Electrically induced calcium elevation, activation, and parthenogenetic development of bovine oocytes. *Mol. Reprod. Dev.* **34**, 212-23.

Conover, J. C. and Gwatkin, R. B. L. (1988). Pre-loading of mouse oocytes with DNA-specific fluorochrome (Hoechst 33342) permits rapid detection of sperm-oocyte fusion. *J. Reprod. Fert.* **82**, 681-690.

Creton, R. and Jaffe, L. F. (1995). Role of calcium influx during the latent period in sea urchin fertilization. *Dev. Growth. Differ.* **37**, 703-709.

Cuthbertson, K. S. and Cobbold, P. H. (1985). Phorbol ester and sperm activate mouse oocytes by inducing sustained oscillations in cell Ca^{2+}. *Nature* **316**, 541-542.

Dupont, G., McGuinness, O. M., Johnson, M. H., Berridge, M. J. and Borgese, F. (1996). Phospholipase C in mouse oocytes: characterization of beta and gamma isoforms and their possible involvement in sperm-induced Ca^{2+} spiking. *Biochem. J.* **316**, 583-591.

Fabiato, A. (1985). Spontaneous versus triggered contractions of 'calcium-tolerant' cardiac cells from the adult rat ventricle. *Basic Res. Cardiol.* **80**, 83-87.

Fissore, R. A. and Robl, J. M. (1992). Intracellular Ca^{2+} response of rabbit oocytes to electrical stimulation. *Mol. Reprod. Dev.* **32**, 9-16.

Flanagan, J. M., Wall, J. S., Capel, M. S., Schneider, D. K. and Shanklin, J. (1995). Scanning transmission electron microscopy and small-angle scattering provide evidence that native Escherichia coli ClpP is a tetradecamer with an axial pore. *Biochemistry* **34**, 10910-10917.

Florman, H.M., Arnoult, C., Kazam, I.G., Li, C. and O'Toole, C. M. B. (1998). A perspective on the control of mammalian fertilization by egg-activated into channels in sperm: a tale of two channels. *Biol. Reprod.* **59**, 12-16.

Fulton, B. P. and Whittingham, D. G. (1978). Activation of mammalian oocytes by intracellular injection of calcium. *Nature* **273**, 149-151.

Gilkey, J. C. (1983). Roles of calcium and pH in activation of eggs of the medaka fish, Oryzias latipes. *J. Cell. Biol.* **97**, 669-678.

Heffner, L. J. and Storey, B. T. (1981). The role of calcium in maintaining motility in mouse spermatozoa. *J. Exp. Zool.* **218**, 427-434.

Jaffe, L. F. (1980). Calcium explosions as triggers of development. *Ann. N. Y. Acad. Sci.* **339**, 86-101.

Jaffe, L. F. (1983). Sources of calcium in egg activation: a review and hypotheses. *Dev. Biol.* **99**, 256-276.

Jaffe, L. F. (1990). The roles of intermembrane calcium in polarising and activating eggs. In *Mechanism of Fertilization*. Nato ASI Series Vol. H45. (ed. B. Dale), pp. 389-417. Springer-Verlag Berlin.

Jaffe, L. F. (1991). The path of calcium in cytosolic calcium oscillations: a unifying hypothesis. *Proc. Natl. Acad. Sci. USA.* **88**, 9883-9887.

Jones, K. T., Carroll, J., Merriman, J. A., Whittingham, D. G. and Kono, T. (1995). Repetitive sperm-induced Ca^{2+} transients in mouse oocytes are cell cycle dependent. *Development* **121**, 3259-3266.

Jones, K. T. and Whittingham, D. G. (1996). A comparison of sperm- and IP$_3$-induced Ca^{2+} release in activated and aging mouse oocytes. *Dev. Biol.* **178**, 229-237.

Kimura, Y., Yanagimachi, R., Kuretake, S., Bortkiewicz, H., Perry, A.C.F. and Yanagimachi, H. (1998). Analysis of mouse oocyte activation suggests the involvement of sperm perinuclear material. *Biol. Reprod.* **58**, 1407-1415.

Kline, D. (1988). Calcium-dependent events at fertilization of the frog egg: injection of a calcium buffer blocks ion channel opening, exocytosis, and formation of pronuclei. *Dev. Biol.* **126**, 346-361.

Kline, D. and Kline, J. T. (1992). Repetitive calcium transients and the role of calcium in exocytosis and cell cycle activation in the mouse egg. *Dev. Biol.* **149,** 80-89.

Kubota, H. Y., Yoshimoto, Y., Yoneda, M. and Hiramoto, Y. (1987). Free calcium wave upon activation in Xenopus eggs. *Dev. Biol.* **119**, 129-136.

Lawrence, Y., Whitaker, M., and Swann, K. (1997). Sperm-oocyte fusion is the prelude to the initial Ca^{2+} increase at fertilization in the mouse. *Development* **124**, 233-241.

Longo, F. J., Lynn, J. W., McCulloh, D. H. and Chambers, E. L. (1986). Correlative ultrastructural and electrophysiological studies of sperm-egg interactions of the sea urchin, Lytechinus variegatus. *Dev. Biol.* **118,** 155-66.

McDougall, A., Sardet, C. and Lambert, C. C. (1995). Different calcium-dependent pathways control fertilisation-triggered glycoside release and the cortical contraction in ascidian eggs. *Zygote* **3**, 251-258.

McGuinness, O. M., Moreton, R. B., Johnson, M. H. and Berridge, M. J. (1996). A direct measurement of increased divalent cation influx in fertilised mouse oocytes. *Development* **122**, 2199-2206.

McNiven, A. I., Yoshida, S., Georgiou, P. and House, C. R. (1988). A delayed all-or-none hyperpolarisation induced by a single Ca action potential in hamster eggs. *Pflugers. Arch.* **412**, 451-453.

Miyazaki, S., Hashimoto, N., Yoshimoto, Y., Kishimoto, T., Igusa, Y. and Hiramoto, Y. (1986). Temporal and spatial dynamics of the periodic increase in intracellular free calcium at fertilization of golden hamster eggs. *Dev. Biol.* **118**, 259-267.

Miyazaki, S., Yuzaki, M., Nakada, K., Shirakawa, H., Nakanishi, S., Nakade, S. and Mikoshiba, K. (1992). Block of Ca^{2+} wave and Ca^{2+} oscillation by antibody to the inositol 1,4,5-trisphosphate receptor in fertilized hamster eggs. *Science* **257**, 251-255.

Myles, D. G. (1993). Molecular mechanisms of sperm-egg membrane binding and fusion in mammals. *Dev. Biol.* **158,** 35-45.

Ozil, J.-P. and Swann, K. (1995). Stimulation of repetitive calcium transients in mouse eggs. *J. Physiol. (Lond.)* **483,** 331-346.

Parrington, J., Swann, K., Shevchenko, V. I., Sesay, A. K. and Lai, F. A. (1996). Calcium oscillations in mammalian eggs triggered by a soluble sperm protein. *Nature* **379,** 364-368.

Primakoff, P., Hyatt, H. and Tredick-Kline, J. (1987). Identification and purification of a sperm surface protein with a potential role in sperm-egg membrane fusion. *J. Cell. Biol.* **104**, 141-149.

Quinn, P., Barros, C. and Whittingham, D. G. (1982). Preservation of hamster oocytes to assay the fertilizing capacity of human spermatozoa. *J. Reprod. Fert.* **66**, 161-168.

Rochwerger, L., Cohen, D. J. and Cuasnicu, P. S. (1992). Mammalian sperm-egg fusion: the rat egg has complementary sites for a sperm protein that mediates gamete fusion. *Dev. Biol.* **153**, 83-90.

Sauer, H., Pratsch, L. Tschopp, J., Bhakdi, S. and Peters, R. (1991). Functional size of complement and perforin pores compared by confocal laser scanning microscopy and fluorescence microphotolysis. *Biochim. Biophys. Acta* **1063**, 137-146.

Schmidt, T., Patton, C. and Epel, D. (1982). Is there a role for the Ca^{2+} influx during fertilization of the sea urchin egg? *Dev. Biol.* **90**, 284-90.

Schultz, R. M. and Kopf, G. S. (1995). Molecular basis of mammalian egg activation. *Curr. Top. Dev. Biol.* **30**, 21-62.

Sette, C., Bevilacqua, A., Bianchini, A., Mangia, F., Geremia, R. and Rossi, P. (1997). Parthenogenetic activation of mouse eggs by microinjection of a truncated c-kit tyrosine kinase present in spermatozoa. *Development* **124**, 2267-2274.

Soeller, C. and Cannell, M. B. (1996). Construction of a two-photon microscope and optimisation of illumination pulse duration. *Pflugers Arch.* **432**, 555-561.

Sun, F. Z., Hoyland, J., Huang, X., Mason, W. and Moor, R. M. (1992). A comparison of intracellular changes in porcine eggs after fertilization and electroactivation. *Development* **115,** 947-956.

Swann, K. and Whitaker, M. (1986). The part played by inositol trisphosphate and calcium in the propagation of the fertilization wave in sea urchin eggs. *J. Cell. Biol.* **103**, 2333-2342.

Swann, K. and Lai, F. A. (1997). A novel signalling mechanism for

generating Ca^{2+} oscillations at fertilization in mammals. *BioEssays* **19**, 371-378.

Swann, K., Igusa, Y. and Miyazaki, S. (1989). Evidence for an inhibitory effect of protein kinase C on G-protein-mediated repetitive calcium transients in hamster eggs. *EMBO J.* **8**, 3711-3718.

Takamatsu, T. and Wier, W. G. (1990). High temporal resolution video imaging of intracellular calcium. *Cell Calcium* **11,** 111-120.

Visconti, P.E. and Kopf, G.S. (1998). Regulation of protein phosphorylation during sperm capacitation. *Biol. Reprod.* **59**, 1-6.

Whitaker, M. and Swann, K. (1993). Lighting the fuse at fertilization. *Development* **117**, 1-12.

Whitaker, M., Swann, K., Crossley, I. (1989). What happens during the latent period at fertilization. In *Mechanisms of Egg Activation: Plants to Humans* (ed. R. Nuccitelli), Nato ASI Series, Vol. H45, pp. 157-171. New York: Springer.

Wier, W. G. and Blatter, L. A. (1991). Ca(2+)-oscillations and Ca(2+)-waves in mammalian cardiac and vascular smooth muscle cells. *Cell Calcium* **12,** 241-254.

Wolfsberg, T. G and White, J. M. (1996). ADAMs in fertilization and development. *Dev. Biol.* **180,** 389-401.

Wolosker, H., Kline, D., Bian, Y., Blackshaw, S., Cameron, A. M., Fralich, T. J., Schnaar, R. L. and Snyder, S. H. (1998). Molecularly cloned mammalian glucosamine-6-phosphate deaminase localizes to transporting epithelium and lacks oscillin activity. *FASEB J.* **12,** 91-99.

Wyke, A.M., Impraim, C.C., Knutton, S. and Pasternak, C.A. (1980). Components involved in virally mediated membrane fusion and permeability changes. *Biochem. J.* **190**, 625-638.

Yanagimachi, R. (1978). Calcium requirement for sperm-egg fusion in mammals. *Biol. Reprod.* **19**, 949-958.

Yanagimachi, R. (1994). Mammalian fertilization. In *The Physiology of Reproduction, Second Series.* (ed E. Knobil and J. D. Neill), pp. 189-317. New York: Raven Press, Ltd.

Zucker, R. S., Steinhardt, R. A. and Winkler, M. M. (1978). Intracellular calcium release and the mechanisms of parthenogenetic activation of the sea urchin egg. *Dev. Biol.* **65,** 285-295.